

Supporting Information

A Dual-Reporter System for Real-Time Monitoring of SARS-CoV-2 Main Protease Activity in Live Cells Enables Identification of an Allosteric Inhibition Path.

Authors: Yaron Bram^{1,7}, Xiaohua Duan^{2,7}, Benjamin E. Nilsson-Payant^{3,6,7}, Vasuretha Chandar¹, Hao Wu^{4,7}, Derek Shore^{4,7}, Alvaro Fajardo⁵, Saloni Sinha¹, Nora Hassan¹, Harel Weinstein^{4*}, Benjamin R. TenOever^{3,5*}, Shuibing Chen^{2,*}, Robert E. Schwartz^{1,4,8,*}.

¹ Division of Gastroenterology and Hepatology, Department of Medicine, Weill Cornell Medicine, 1300 York Ave, New York, NY 10065, USA

² Department of Surgery, Weill Cornell Medicine, 1300 York Ave, New York, NY 10065, USA

³ Department of Microbiology, Icahn School of Medicine at Mount Sinai, One Gustav L Levy Place, New York, NY 10029, USA

⁴ Department of Physiology, Biophysics, Weill Cornell Medicine, 1300 York Ave, New York, NY 10065, USA

⁵ Current location: Department of Microbiology, New York University, New York, NY 10016, USA.

⁶ Current location: TWINCORE Centre for Experimental and Clinical Infection Research, Institute for Experimental Virology, 30625 Hannover, Germany.

⁷ These authors contributed equally.

⁸ Lead Contact

* Correspondence: haw2002@med.cornell.edu (H.W.), Benjamin.tenOever@NYUlangone.org (B.T.), shc2034@med.cornell.edu (S.C.), res2025@med.cornell.edu (R.E.S.).

SUPPLEMENTARY TABLES

Table S1. Protease inhibitors used in this study.

Table S2. 3CL^{pro} Inhibitors identified in the cell reporter chemical screen.

Table S3. Sequences of the primers used for qRT-PCR in this study.

Table S4. Inhibitors binding free energy (BFE).

Table S5. 3CL^{pro} alanine substitution inhibition analysis.

Table S6. Coordination information of decoy sites.

Table S7. Idazoxan-S' coordination information.

SUPPLEMENTARY FIGURES

Figure S1. Fluorescent images 3CL^{pro} cell-reporter with different NSP's junction sequences.

Figure S2. 3CL^{pro} cell reporter activity quantification with calpain inhibitors.

Figure S3. Chemical screen lead compounds IC₅₀ quantification using *In-vitro* FRET assay.

Figure S4. Inhibitors interactions with 3CL^{pro} catalytic site.

Figure S5. Inhibitors interactions with 3CL^{pro} dimerization site.

Figure S6. Structural definition of 3CL^{pro} arbitrary sites used for comparison.

Table S1 Protease Inhibitors

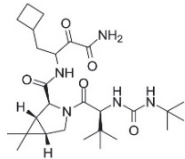
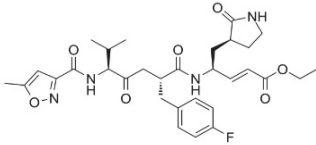
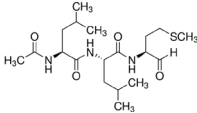
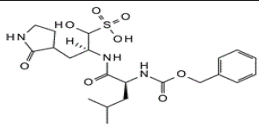
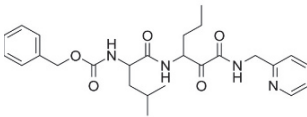
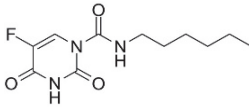
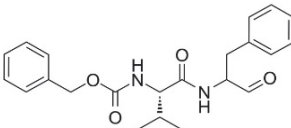
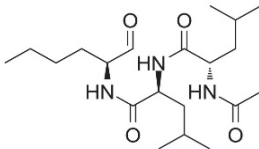
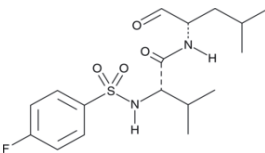
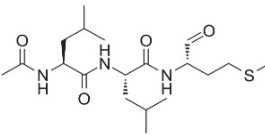
Boceprevir	Selleck Chemicals	S3733	
Rupintrivir	Tocris	6414	
Calpain inhibitor II	Sigma-Aldrich	208722	
GC376	Carbosynth	BG167367	
Calpain Inhibitor XII	Cayman Chemical	14466	
Carmofur	Sigma-Aldrich	C1494	
MDL28170	Tocris	1146	
ALLN	Santa Cruz Biotech	sc-221236	
Calpain Inhibitor VI	Santa Cruz Biotech	sc-293979	
ALLM	Sigma-Aldrich	208721	

Table S2 3Cl^{Pro} Inhibitors

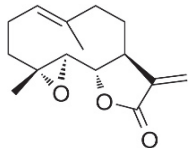
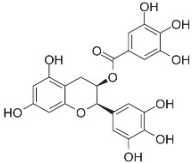
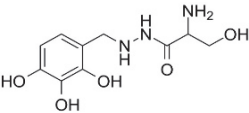
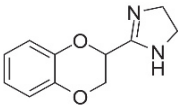
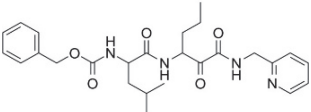
Parthenolide	Sigma-Aldrich	P0667	
EGCG	Sigma-Aldrich	E4143	
Benserazide	Sigma-Aldrich	B7283	
Idazoxan	Sigma-Aldrich	I6138	
Mundulone	MicroSource	14466	

Table S3. qPCR primers

Primer name	Sequence
18s-Forward	GGCCCTGTAATTGGAATGAGTC
18s-Reverse	CCAAGATCCAACACTACGAGCTT
SARS-CoV-2-TRS-L	CTCTTGTAGATCTGTTCTCTAAACGAAC
SARS-CoV-2-TRS-N	GGTCCACCAAACGTAATGCG
GLuc-Forward	TCTGATCTGCCTGTCCCACATCAAG
GLuc-Reverse	CCAGGAATCTCAGGAATGTGCGACGA

Table S4.

3CL^{pro} inhibitors binding free energy (BFE)

Compound	Catalytic site		Dimer interface	
	Total binding free energy (BFE)	Residue w/ largest decomposed BFE	Total binding free energy (BFE)	Residue w/ largest decomposed BFE
Benserazide-R (BEN-R)	-10.6	E166 (-5.4)	0.4	D289 (-3.1)
Benserazide-S (BEN-S)	-17.4	C44 (-6.1)	-5.6	E166 (-4.3)
EGCG	-21.5	C145 (-3.5)	-21.8	C128 (-3.3)
Idazoxan-R (IDX-R)	-19.0	C44 (-1.8)	-17.7	S284 (-1.6)
Idazoxan-S (IDX-S)	-11.0	C44 (-1.2)	-16.0	S284 (-1.0)
Mundulone-R (MND-R)	-24.4	D187 (-2.5)	-21.0	R4 (-2.2)
Mundulone-S (MND-S)	-16.1	H41 (-1.4)	-23.5	R4 (-5.7)
Parthenolide (PRT)	-13.1	M165 (-1.3)	-28.0	Q299 (-2.2)
				F291 (-1.1)
				F3 (-0.8)
				K137 (-1.9)
				M6 (-1.4)
				F291 (-1.7)

All energy values are in the unit of kcal/mol

Table S5. 3C1^{pro} alanine substitution analysis

Compound	WT	Catalytic Site			Dimer Interface		
		C44A	M165A	D187A	R4A	E288A	Q299A
Benserazide	65.78	137.2	* n.i	**	* n.i	40.3	174.10
EGCG	11.91	189.70	71.10		48.24	42.58	9.36
Idazoxan	21.31	42.71	104.03		* n.i	22.53	111.20
Mundulone	0.62	4.88	13.59		3.67	2.376	9.36
Parthenolide	1.22	4.68	5.58		4.01	6.59	15.21
* no inhibition, ** inactive enzyme							
IC50 (μM)							

Table S6. Coordination information among decoy sites

A

		Apo NSP5			Parthenolide-bound NSP5		
		Total correlation	DBS	CI (NCI)	Total correlation	DBS	CI (NCI)
Coordinated	D1_A	15.0	0.8 (6%)	1.7 (11%)	20.9	1.1 (5%)	3.0 (14%)
	D2_A	12.0	1.1 (10%)	1.1 (9%)	15.4	1.1 (7%)	1.5 (10%)
	D3_A	17.8	1.9 (11%)	1.0 (6%)	17.7	2.0 (11%)	0.7 (4%)
	D1_B	16.9	1.7 (10%)	1.3 (8%)	19.8	1.1 (5%)	0.8 (4%)
	D2_B	10.9	1.3 (12%)	1.1 (10%)	15.7	0.7 (5%)	1.0 (7%)
	D3_B	18.0	1.5 (8%)	1.4 (8%)	19.9	1.6 (8%)	2.3 (12%)

B

		Apo NSP5			Parthenolide-bound NSP5		
		Total correlation	DBS	CI (NCI)	Total correlation	DBS	CI (NCI)
Coordinated	D1_A	15.0	0.8 (6%)	1.7 (11%)	20.9	1.1 (5%)	3.0 (14%)
	D2_A	12.0	1.1 (10%)	1.1 (9%)	15.4	1.1 (7%)	1.5 (10%)
	D3_A	17.8	1.9 (11%)	1.0 (6%)	17.7	2.0 (11%)	0.7 (4%)
	D1_B	16.9	1.7 (10%)	1.3 (8%)	19.8	1.1 (5%)	0.8 (4%)
	D2_B	10.9	1.3 (12%)	1.1 (10%)	15.7	0.7 (5%)	1.0 (7%)
	D3_B	18.0	1.5 (8%)	1.4 (8%)	19.9	1.6 (8%)	2.3 (12%)

* Normalized CI (NCI) by coordinated sites' total correlation are shown in parentheses.

Table S7. Idazoxan-S' coordination information

Idazoxan-S-bound NSP5					
			Coordinators		
			CI (NCI)		
		Total correlation	DBS	OR_apo	OR_holo
Coordinated	DBS	19.9	N/A	4.3 (22%)	4.6 (23%)
	OR_apo	25.0	7.4 (30%)	N/A	N/A
	OR_holo	30.6	9.3 (30%)	N/A	N/A

* Percentages of CI in coordinated sites' total correlation (normalized CI) are shown in parentheses

** CI of one site itself is 100% and not shown. OR_apo and OR_holo have many shared residues so their mutual CIs are not shown.

Fig. S1.

3CL^{pro} cleavage efficiency of NSP's junction sequences.

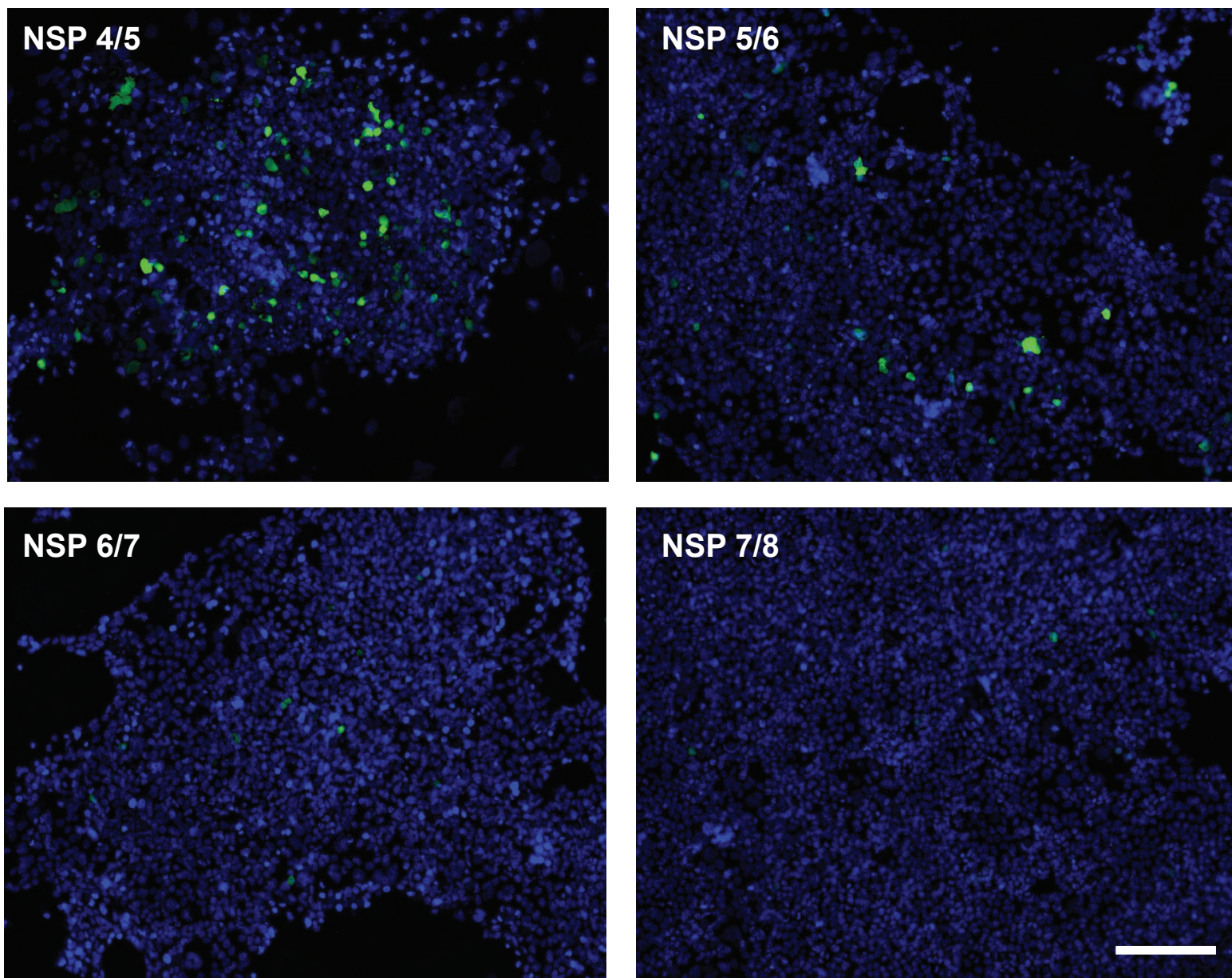


Figure S1: Representative fluorescence images of citrine expression in HEK293T cells 24h after transfection with different 3CL^{pro} linkers corresponding to the viral NSP's junction sites. Scale bar, 100 μ m

Fig. S2.

Calpain inhibitors effect on 3CL^{pro} activity

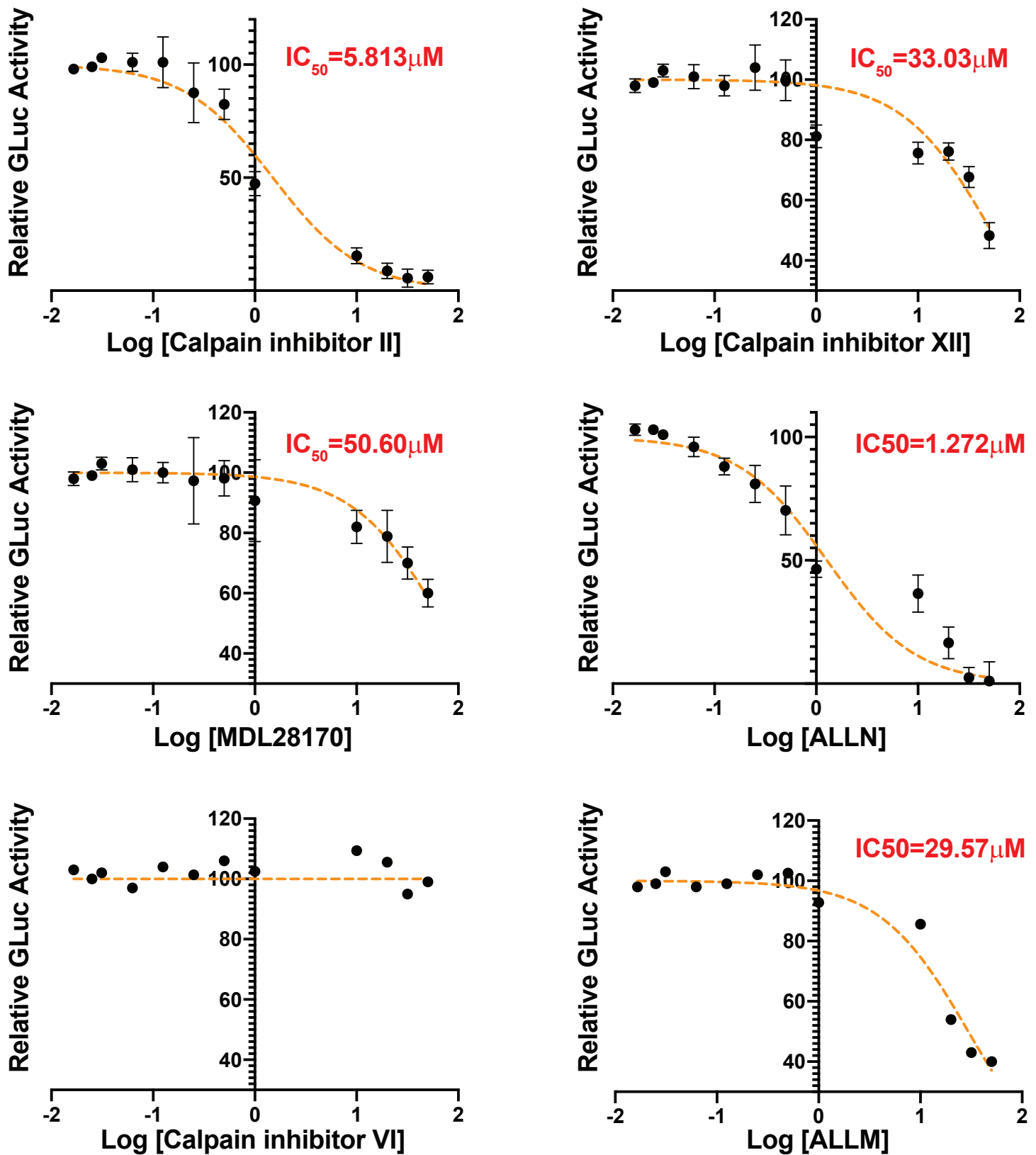


Figure S2. Each compound was tested in multiple concentrations, luminescent signal was recorded 48 h after compound addition and inhibition was calculated as the percentage of luminescent signal compared to the vehicle treated group. Data is plotted as mean ± SD, N=3 for each concentration point, nonlinear correlation analysis was used to evaluate compounds IC₅₀.

Fig. S3.
3CL^{pro} *In-vitro* inhibition assay

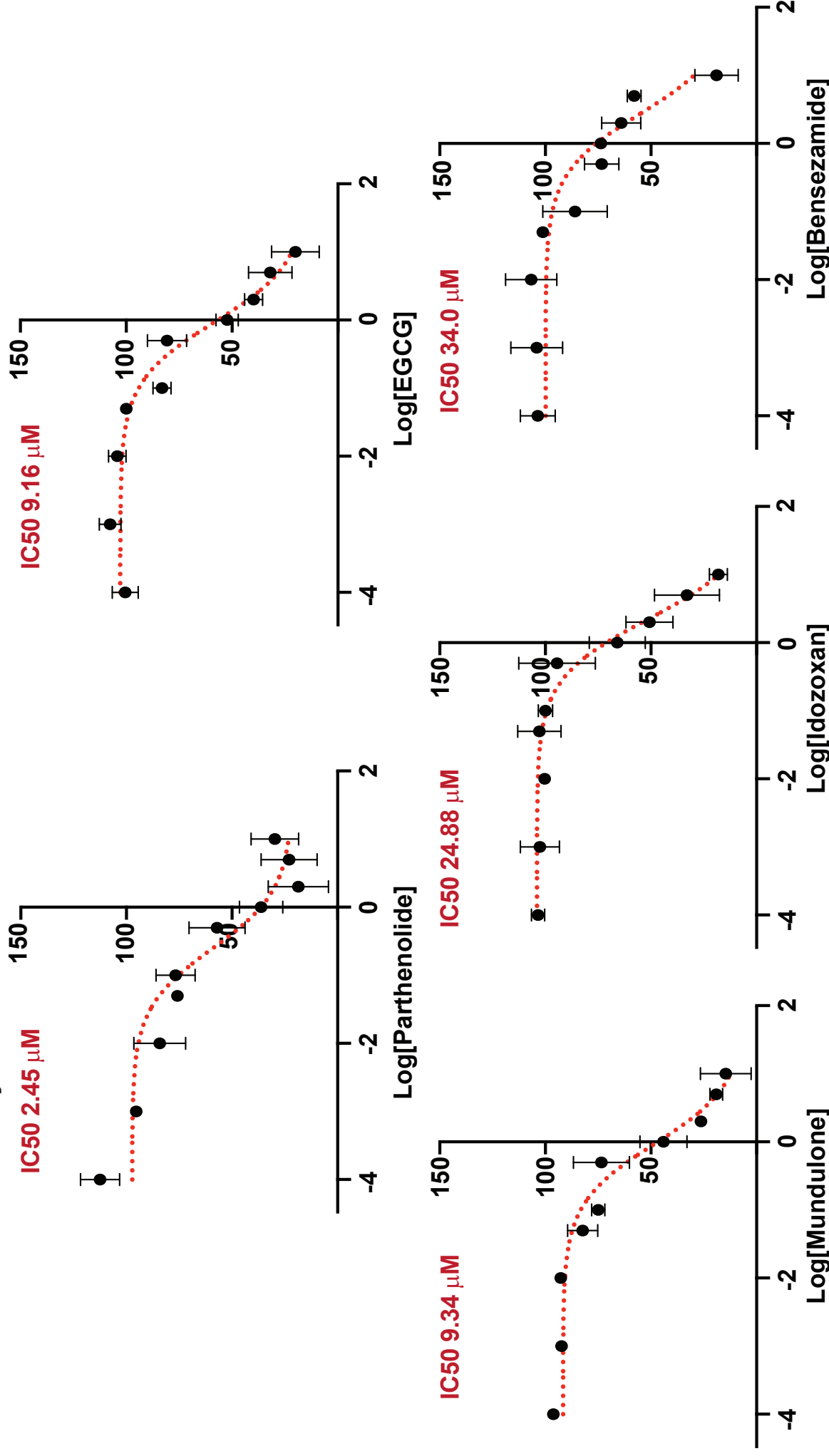


Figure S3. 3CL^{pro} was incubated with each of the compounds in multiple concentrations (1hr, 25°C), followed by the addition of FRET peptide substrate. Protease activity was calculated as the relative fluorescent signal compared to the vehicle treated group (Ex 485, Em 525). Data is plotted as mean ± SD, N=3 for each concentration point, nonlinear correlation analysis was used to evaluate compounds IC₅₀.

The modes of inhibitor binding in the catalytic site of 3CL^{pro}

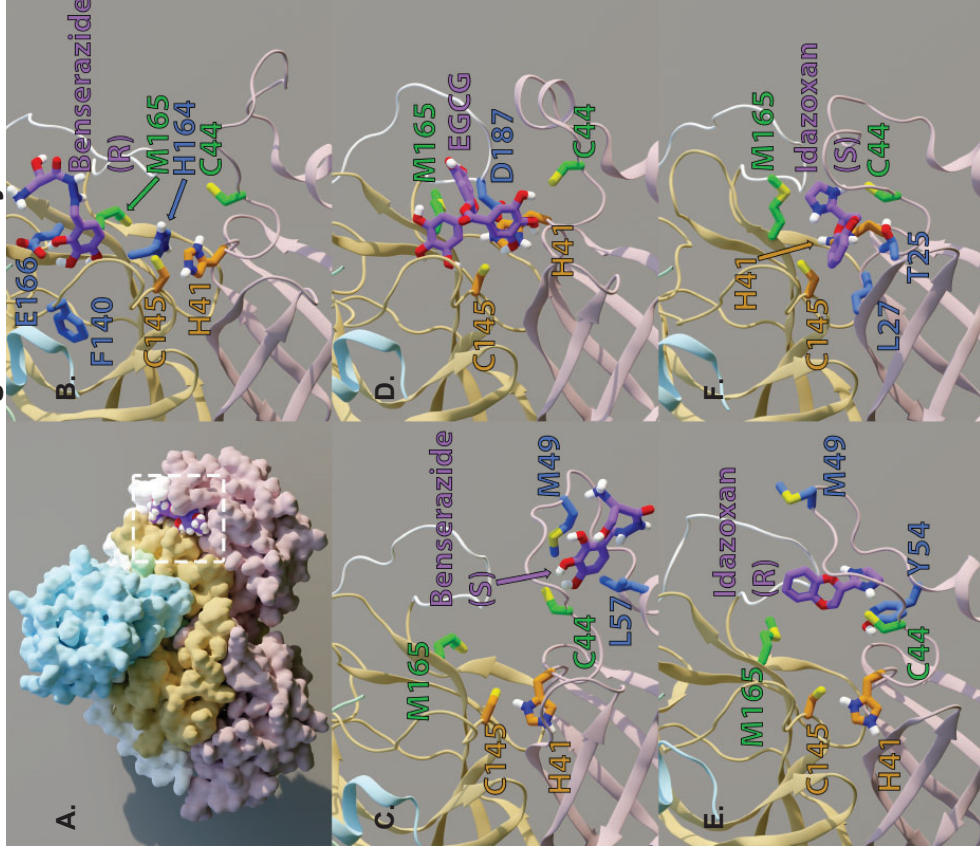


Fig. S4.

Figure S4 .(A) 3CL^{pro} is shown in surface; D1 (pink); D2 (yellow); D3 (light blue); N-finger (mint); linker loop (white); Mundulone (R-enantiomer, purple). **(B-F)** Inhibitor binding modes: as in Figure 6; residues probed by mutagenesis (green); catalytic residues (orange); residues with large contribution to calculated enzyme-inhibitor binding free energy (BFE, blue). **(B)** Benserazide (R-enantiomer); **(C)** Benserazide (S-enantiomer); **(D)** EGCG; **(E)** Idazoxan (R-enantiomer); **(F)** Idazoxan (S-enantiomer).

Fig. S5 Dimerization site docking poses

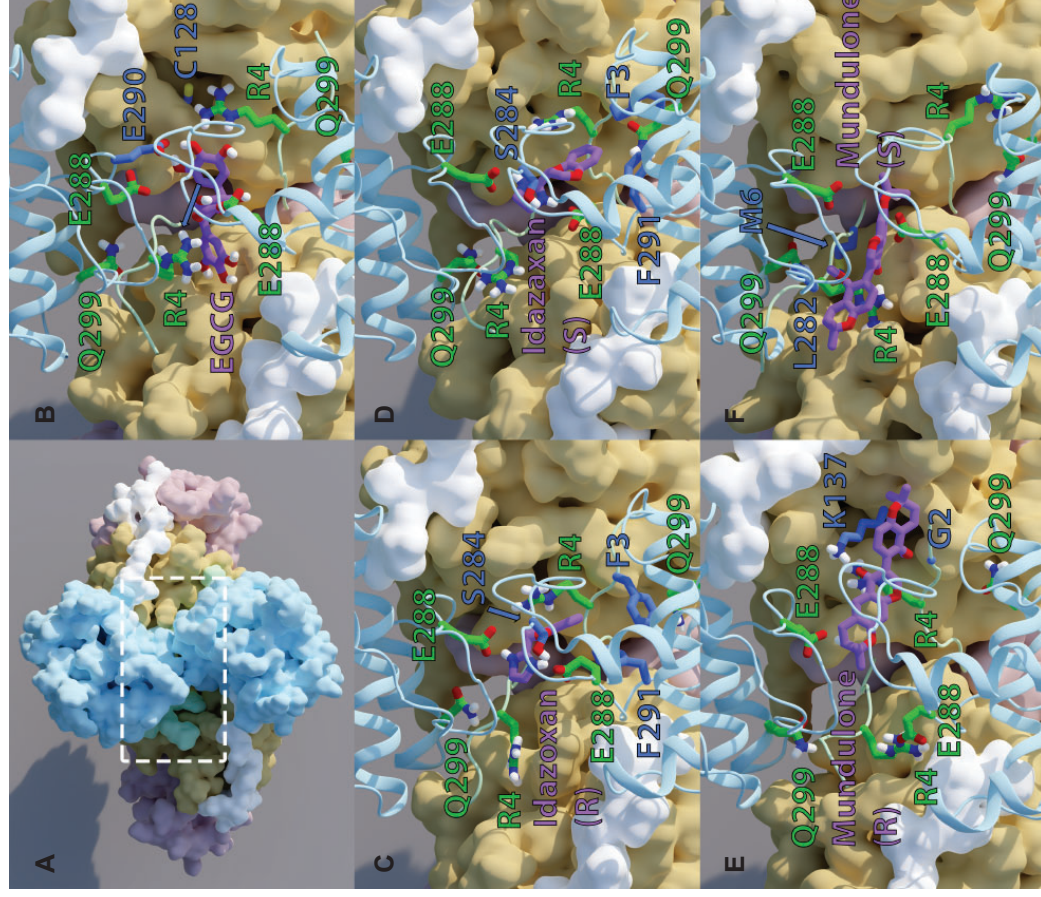


Figure S5.(A) 3CL^{pro} is shown in surface; Domain 1 is pink; Domain 2 is yellow; Domain 3 is light blue; N-finger is mint; Linker loop is white. (B-F) Inhibitors binding modes: as in Figure 7, inhibitor is shown in purple; residues probed by mutagenesis are green; residues that are predicted to form important interactions with inhibitor are shown in blue. (B) EGCG; (C) Idazoxan (R-enantiomer); (D) Idazoxan (S-enantiomer); (E) Mundulone (R-enantiomer); (F) Mundulone (S-enantiomer)

Fig. S6 Structural definition of decoy sites

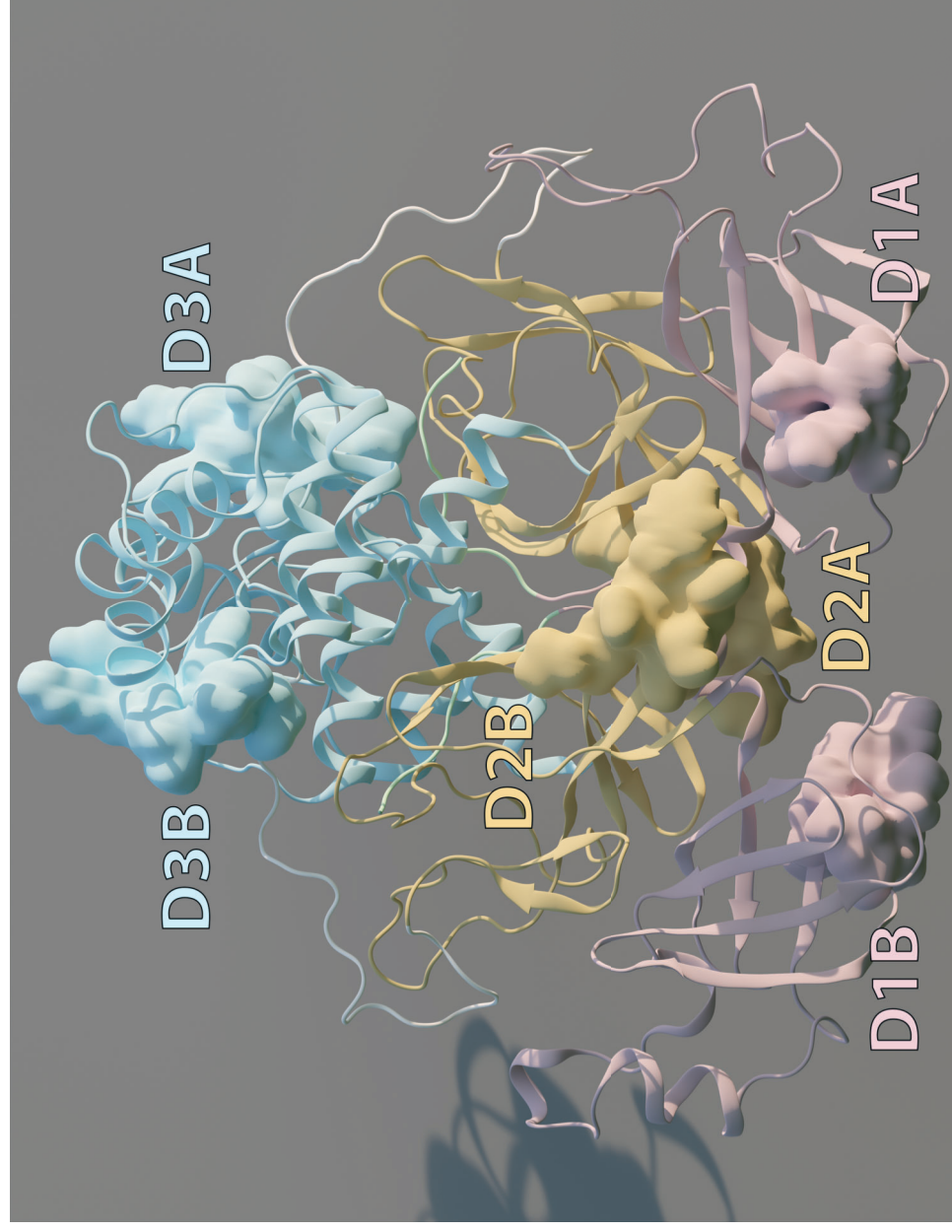


Figure S6. D1 is shown in pink (residues 69-75); D2 is shown in yellow (residues: 151-157); D3 is shown in light blue (residues: 235-241); decoy sites for protomers A and B are labeled accordingly.